Cellular Therapy and Transplantation (CTT). Vol. 13, No. 2, 2024
doi: 10.18620/ctt-1866-8836-2024-13-2-58-64
EDN: FNAWWR
Submitted: 27 March 2024, accepted: 15 June 2024

Dynamics in parameters of the blood matrix metalloproteinases/inhibitors system in the treatment of experimental tuberculous osteitis

Dilyara S. Esmedelyaeva [1], Nina P. Alekseeva [2], Marina E. Dyakova [1], Natalya Yu. Semenova [3], Viktor A. Korzhikov-Vlakh [2], Evgenia G. Korzhikova-Vlakh [4], Tatiana I. Vinogradova [1], Petr K. Yablonsky [1,2]

[1] St. Petersburg Research Institute of Phthisiopulmonology of the Ministry of Health of Russian Federation, St. Petersburg, Russia
[2] St. Petersburg State University, St. Petersburg, Russia
[3] Russian Research Center for Hematology and Transfusiology, St. Petersburg, Russia
[4] Institute of Macromolecular Compounds of Russian Academy of Sciences, St. Petersburg, Russia

Dr. Dilyara S Esmedelyaeva, Polytechnical st. 32, St. Petersburg, Russia
Phone: +7 (921) 183-50-35
E-mail: diljara-e@yandex.ru

Citation: Esmedelyaeva DS, Alekseeva NP, Dyakova ME et al. Dynamics in parameters of the blood matrix metalloproteinases/inhibitors system in the treatment of experimental tuberculous osteitis. Cell Ther Transplant 2024; 13(2): 58-64.

Summary

Imbalance of bone homeostasis is associated with disorders in the of nuclear factor-κB RANK/RANKL/osteoprotegerin (OPG) activating system mediated by matrix metalloproteinases (MMPs). The aim of this work was to evaluate relative dynamics of (MMPs) and their tissue inhibitor (TIMP) in peripheral blood during development of tuberculous osteitis (TO) in rabbit experimental model (n = 32): non-treated infectious control (group 1), and two experimental (treated) groups in which necrectomy, anti-tuberculosis treatment and replacement plastic surgery was performed by means of autografting (group 2), or 3D-printed composite scaffolds (group 3). Serum levels of MMP-3 and MMP-9, their tissue inhibitor (TIMP-1), receptor activator of nuclear factor-κB ligand (RANKL), nonspecific alkaline phosphatase (ALPL), serum albumin (AL), ceruloplasmin (CP), neutrophil elastase (NE) and adenosine deaminase (ADA) were determined before infection and 18 days, 2, 4 and 6 months after the infection. Osteogenesis was evaluated on the basis of microcomputed tomography (micro-CT) and pathohistological examination of bone tissue in control and experimental groups. At the stage of verified tuberculosis osteitis, we have detected a decrease in RANKL (p = 0.017) and AL (p = 0.04), along with increase in TIMP-1 (p = 0.04), CP (p = 0.0004) and NE (p = 0.02), with no changes in ALPL, ADA, and MMP-3 and MMP-9. In group 1 (infection control), foci of specific damage persisted and no signs of bone regeneration were detectable. Both experimental groups exhibited a progressing bone regeneration with the lowest osteodestruction scores in group 2 treated by autografting. The level of inflammatory response increased with progressing infection and declined upon combined treatment. The RANKL levels did not change within 2-6 months. Based on the differences in ALPL and TIMP-1, the use of composite material for plastic surgery was characterized by slower osteointegration and reparative osteogenesis compared to the use of autograft.

Keywords

Bone tuberculosis, matrix metalloproteinases, autografting, biocomposite scaffolds, plastic surgery, biomaterials, bone regeneration.

Introduction

The key symptom of tuberculous osteitis (TO) is a disorder of bone homeostasis caused by *Mycobacterium tuberculosis* (MTB). The TO treatment includes excision of necrotic bone tissue followed by implantation of replacement material. In the modern concept of reconstructive surgery in bone tuberculosis, an important role is given to the search for new substituting materials with osteoconductive and/or osteoinductive properties as an alternative for the conventionally used autografts [1-4].

It is little known about immune mechanisms of TO. MTB infection induces secretion of chemokines (e.g., IL-8, IP-10 and MCP-1) by osteoblasts leading to leukocyte recruitment, thus promoting bone destruction [5,6]. An imbalance in bone homeostasis is associated with abnormalities in the signaling network including RANK, RANKL and osteoprotegerin (OPG) [7]. RANKL is expressed by osteoblast cell lineage and binds to different receptors, with OPG being the first, followed by RANK expression on the surface of osteoclasts. OPG is a natural antagonist of RANKL. By blocking the RANKL/RANK binding, it may suppress biological effects of RANKL such as bone resorption, osteoclast differentiation, activation and induction of apoptosis [8,9]. In some studies, activation of RANKL has been reported in patients with spinal tuberculosis [10].

Matrix metalloproteinases (MMPs) comprise a family of zinc-dependent proteinases that mediate the action of the RANLK/RANK/OPG system. MMPs are involved in a wide range of physiological and pathological processes, due to their ability to release bioactive molecules embedded in the extracellular matrix (ECM) [11,12]. By their substrate specificity, MMPs are classified into collagenases (MMP-1, MMP-8), gelatinases (MMP-2, MMP-9), stromelysins (MMP-3, MMP-13), and other proteinase families. MMP levels are determined by the balance between their expression and specific inhibition by tissue inhibitors of metalloproteinases (TIMPs). Enhanced expression of genes such as *MMP-9* and cathepsin K has been observed in osteomyelitis caused by *Staphylococcus aureus* [13]. Combined effect of collagenases, gelatinases and stromelysins determines the role of MMP-dependent ECM degradation as an important factor of osseointegration in surgical treatment of TO [14-17].

Recently, we developed biodegradable composite scaffolds based on poly(ε-caprolactone) (PCL) and modified nanocrystalline cellulose (NCC), and studied their biocompatibility [18] and osteoconductive properties *in vivo* [19]. Usage of 3D-printed composite scaffolds bearing viable adherent mesenchymal stem cells (MSCs) in the bone tuberculosis model did also prove the efficiency of this original material for regeneration of affected bone tissue [20]. However, evaluation of the MMP/TIMP level in blood during tuberculosis treatment of experimental TO by plastic surgery with composite scaffolds and/or bone autografts has not been previously performed. Thus, the aim of this work was to study the MMP/TIMP system for evaluation of treatment efficiency in bone tuberculosis, which included tuberculosis therapy combined with bone regeneration by plastic surgery using autografts and 3D-printed composite scaffolds.

Materials and methods

Experimental model and tuberculosis treatment

The experiments were performed with 32 male Chinchilla rabbits weighing 3.5+0.3 kg (Rappolovo Laboratory Animal Nursery, Kurchatov Institute, Russia). The animals were kept in a certified animal facility at the St. Petersburg Research Institute of Phthisiopulmonology, in accordance with the European Convention for the Protection of Vertebrate Animals Used for Experimental and Other Scientific Purposes (Strasbourg, 1986). The study was authorized by Independent Ethical Committee of St. Petersburg Research Institute of Phthisiopulmonology (protocol No.80.3 of 23.06.2021).

The TO model was carried out by the previously developed protocol [21] using *M. tuberculosis* suspension (standard H37Rv strain) sensitive to any antituberculosis drugs. The animals were infected by *M. tuberculosis* at the dose of 1×10^6 CFU. The suspension of M. Tuberculosis was inoculated in the medial condyle of the right femur of the rabbit. After verification of tuberculosis infection (Diaskintest®, Generium, Russia) and visualization of the foci using Aquilion Prime CT scanner (Toshiba, Japan), the animals were divided into three groups. The infection control (group 1, n=5), was not subjected to necrectomy and treatment. In two experimental groups, etiotropic therapy was administered (isoniazid 10 mg/kg subcutaneously; ethambutol and pyrazinamide, 20 mg/kg intragastrically). 18 days later, the necrectomy of affected bone was performed (n=27). In experimental groups, the bone defect was filled with autograft material (group 2, n=12) or with the 3D-printed composite scaffold with pre-adhered MSCs (group 3, n=15). No animal deaths were observed during the entire observation period.

Composite scaffolds

The 3D-printed composite scaffolds used for implantation were prepared as described in our previous paper [19]. Poly(ε-caprolactone) (PCL) was used as a matrix polymer, and nanocrystalline cellulose (NCC) modified with poly(glutamic acid) was added as a filler. For the 3D-printing, we used a blend which consisted of PCL containing 10 wt% of the filler. Before implantation, rabbit mesenchymal stem cells (MSCs) were seeded on the surface of the 3D-printed composite scaffolds [20]. 3D printing was performed using the GeSim BioScaffolder 3D printer (GeSim, Germany).

Biochemical analysis

Blood serum samples were analyzed before experimental infection, and at different terms of infectious process (18 days, 2, 4 and 6 months). The following parameters were measured: serum concentrations of total protein and albumin assayed by a biochemical analyzer kit (LLC "Eiliton", Russia); ceruloplasmin (CP) measured by Ravin method; neutrophil elastase (NE) activity [22], and adenosine deaminase (ADA) activity [23]. The contents of RANKL (E0289Rb), non-specific alkaline phosphatase ALPL (SEB091Rb), MMP-3 (SEA101Rb), MMP-9 (SEA553Rb) and TIMP-1 (SEA552Rb) were determined by immunoenzymatic method using the reagents purchased from Cloud-Clone Corp. (USA).

Micro-CT and histological analysis

Bone samples were excised in the animals after 2, 4 and 6 months of experiment and were examined with a Skyscan 1172 micro-CT scanner (Bruker microCT, Belgium). A conditional qualitative/quantitative scale (0 to 2 points) was utilized for evaluation of results: 0 means absence of the feature; 1 means the moderate expression of the feature, and 2 means strong expression of the feature. The signs of osteoregeneration (implant visualization, sprouting of bone beams, their composition, structural restoration of cortical closure and epiphyseal plates) and the signs of osteodestruction (presence of bone cavities and microsequestrations) were considered.

Histopathology studies of femoral diaphysis/epiphysis segments included fixation in 10% neutral formalin, decalcification, paraffin embedding, staining of sections with hematoxylin and eosin as well as Ziehl-Nielsen technique (detection of acid-fast mycobacteria). The incidence and activity stage of the specific infiltrates were evaluated. Appropriate technical details can be found in our previous paper [20].

Statistical data processing

Statistica 7.0 software package (StatSoftInc., USA) was used for data processing. After testing for normality of distribution (Shapiro-Wilkie), data were presented as median (Me), first and third quartiles (Q1-Q3). The repeated observations analysis of variance model (ANOVA Repeated Measures) was applied with the assessment of significance (effect) of differences between groups (group factor) and in the dynamics of the experiment (time factor): before infection (0 day) and 18 days, 2, 4 and 6 months after infection, and significant interaction effect of groups and time [24].

Results

At all steps of the study, body mass of animals in group 1 (infected controls) was significantly lower than in the experimental (treated) groups ($p = 0.05$), the time-dependent effect was significant ($p = 0.05$). Evaluation of inflammatory markers 18 days after infection revealed an increase in the median level CP ($p = 0.02$) from 0.34 (0.28; 0.45) g/L to 0.42 (0.35; 0.52) g/L, and a decrease in total protein from 71.00 (66.00; 77.00) g/L to 65.60 (62.50; 60.70) g/L. Neutrophil elastase (NE) activity increased from 293.40 (251.90; 323.30) IU to 347.70 (293.40; 423.80) IU, while ADA values remained unchanged. Evaluation of bone homeostasis markers revealed a decrease in RANKL concentration ($p = 0.03$) from 99.70 (87.50; 102.80) ng/L to 76.70 (57.6; 91.40) ng/L, and a trend toward a decrease in alkaline phosphatase (ALPL) from 0.32 (0.20; 1.10) to 0.13 (0.10; 0.23). There was a decrease in TIMP-1 concentration from 16.47 (10.58; 20.44) to 3.52 (0.40; 11.64) ng/L (p=0.002), with no changes in MMP-3 and MMP-9. Changes in MMP-3 concentration showed positive correlation with MMP-9 (r = 0.45; $p = 0.04$) and negative correlation with TIMP-1 (r = -0.69; $p = 0.001$), suggesting an imbalance in the MMP/TIMP system toward proteolysis, due to decreased MMP inhibitor. Thus, the inflammatory response 18 days after infection was characterized by an increased level of nonspecific inflammatory response, decreased activity of osteoblasts, and a shift in MMP/TIMP system.

Within these terms, we observed a positive reaction to intradermal injection of Diaskintest® in all studied animals (the erythema diameter was 27.73 ± 0.54 mm). With respect to clear biochemical markers of inflammatory response, these findings point to development of a specific inflammatory process and the adequacy of this model for studies of tuberculosis osteitis. Osteodestruction and osteoregeneration processes after 2 to 6 months post-infection were evaluated by micro-CT data (Fig. 1). In the infection control group, no signs of osteoregeneration were detected at any of the study terms, whereas an increase in osteoregeneration was observed in experimental groups, starting from 2 months. The lowest osteodegeneration scores were detected in the group treated by autografting at 6 months.

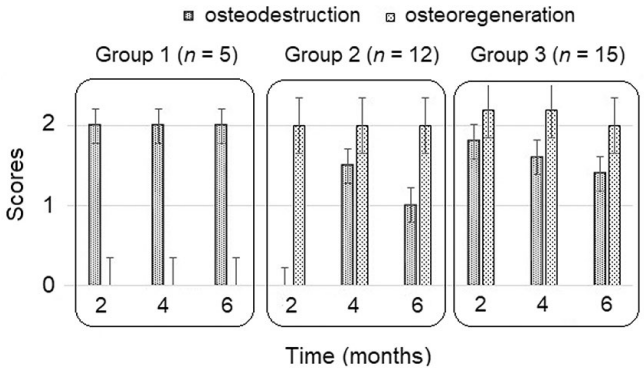

Figure 1. Osteodestruction and bone regeneration scores in the course of infectious process (sum of points based on micro-CT analysis)

According to the histological analysis, in the control group of infection, extensive specific inflammatory-necrotic changes were detected at all periods of observation. At the same time, in group 2 (autografting), no signs of inflammation were found 4 months after infection, while minor signs of inflammation were observed in group 3 during the same period.

Evaluation of the process severity by nonspecific inflammatory markers revealed that the groups differed in concentrations of total albumin ($p = 0.007$) and CP ($p = 0.005$), and their levels changed from 2 to 6 months ($p = 0.004$ and $p = 0.02$, respectively). In group 1, a decrease in total albumin content was detected, whereas such effect was not observed in groups 2 and 3 (Fig. 2a). The increase in CP levels progressed in group 1, while in the experimental groups, after some decrease, the values returned to the initial values (Fig. 2b).

The NE activity differed between the groups ($p = 0.01$) and changed during progression of disease ($p = 0.0003$). At early time points, NE activity in group 1 was lower than in group 3, and it became higher by the 6th month. In group 2, the dynamics of NE changes was less pronounced, and its activity did not differ from initial values (a significant effect of group and time interaction, $p = 0.001$) (Fig. 2c). ADA activity was more pronounced in group 1 and did not differ between experimental groups ($p = 0.72$). Its highest level was observed at 4 months in all groups ($p = 0.006$).

The concentration of ALPL, a cellular marker of osteoblasts, differed between groups (p = 0.002). In group 1, the enzyme level of 0.22 (0.22; 0.22) ng/mL did not change against the initial values, being increased in experimental groups as the function of observation period (time-dependent effect, p = 0.002). At the same time, the ALPL concentration was different in experimental groups thus indicating differences in the degree of bone mineralization. Specifically, in group 2, ALPL concentration exceeded the initial level 3.5 and 4.2 times at 4 and 6 months, respectively. In turn, ALPL increase in group 3 was 1.3- and 2.0-fold at 4 and 6 months, respectively. The concentration of bone metabolism marker, RANKL, did not differ between groups (inter-group effect, p = 0.87) and in the course of observation (time-dependent effect, p = 0.20). In addition, RANKL concentration was not associated with changes of inflammatory response markers.

The concentration of TIMP-1 differed between the groups (p = 0.0002) and changed in the course dynamics of infectious process (p = 0.0003): it decreased in the control infection and increased in the treated experimental groups (Fig. 2d). The highest level of the MMP inhibitor was detected in group 2. Local increase of TIMP-1 was observed earlier, during osteointegration of titanium implants in the femur in rats [25].

Variations of MMP-3 concentration between groups (p = 0.06) and over time were not significant (p = 0.07). However, there was a tendency of its slight increase by the 6th month. MMP-3 level was 1.5 and 2.0 times higher in group 1 compared to groups 2 and 3 (Fig. 3a). In turn, MMP-9 concentration differed between the groups (p = 0.05) and changed in the course of the study (p = 0.05). The most pronounced changes of MMP-9 were observed in the control group. In group 1 the MMP-9 level at the 4th month exceeded that in the groups 2 and 3 by 3.0 and 2.1 times, respectively. By the 6th month, these differences decreased to 1.8 and 2.3 times, respectively (Fig. 3b).

In the pathogenesis of experimental tuberculosis osteitis, clear correlations were found between some markers characterizing different aspects of bone metabolism in experimental groups: RANKL with MMP-9 at 2, 4 and 6 months (r = -0.71, p = 0.02; r = -0.47, p = 0.05; r = -0.59, p = 0.05, n=32) and TIMP-1 (r = 0.63, p = 0.03, n=32) at 6 months; ALPL with CP (r = -0.55, p = 0.01; r = -0.45, p = 0.01, n=32) and TIMP-1 (r = 0.76, p = 0.02; r = 0.95, p = 0.0002, n=32) at 4 and 6 months, respectively. The observed patterns probably indicate a decrease in the inflammatory response and the beginning of peri-implantation bone remodeling in the experimental groups starting from the 2nd month.

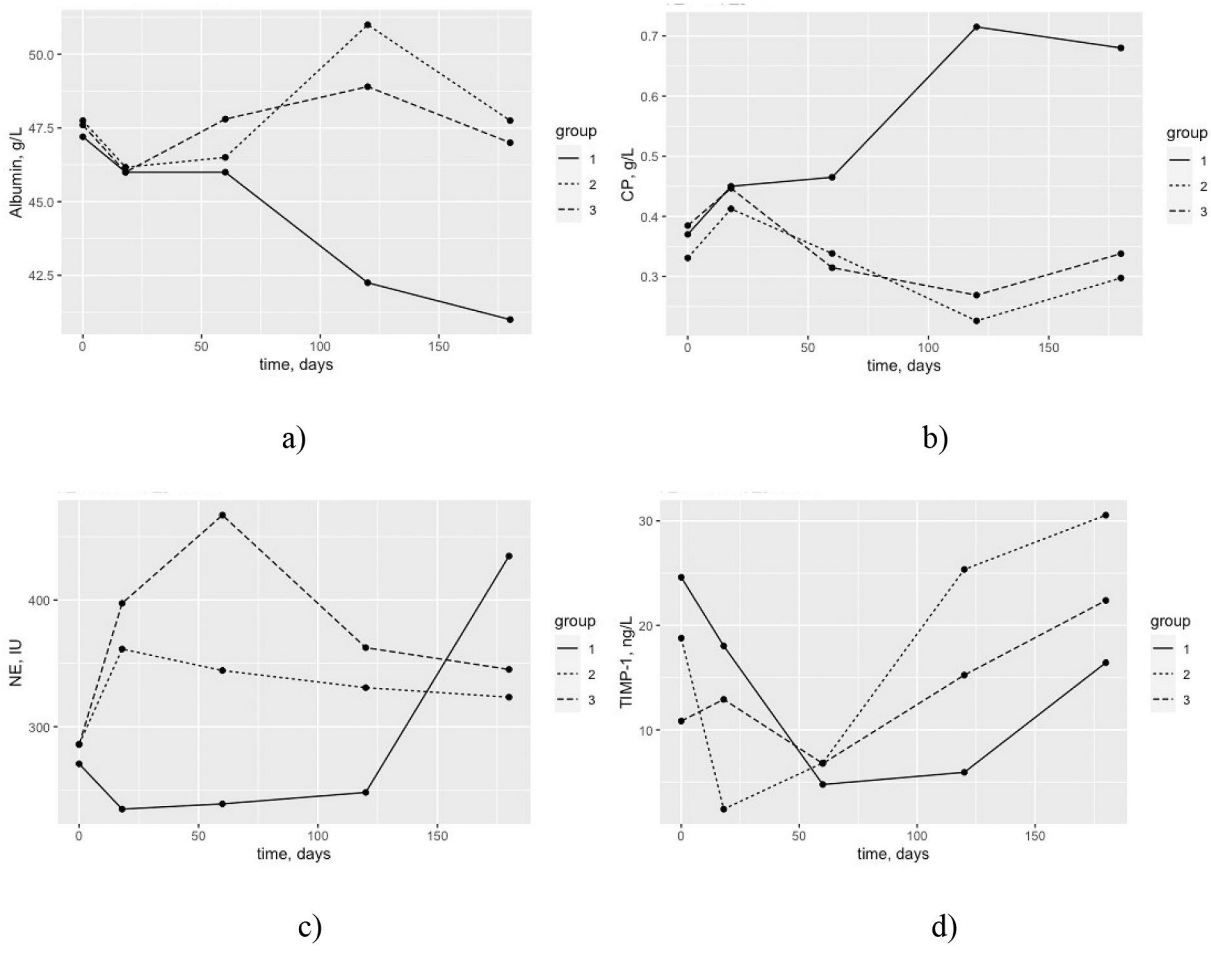

Figure 2. Dynamics of changes in some biochemical markers from the day of infection to 4 months of follow up: (a) Al – albumin concentration; (b) CP ceruloplasmin concentration; (c) NE elastase activity; (d) TIMP-1 – tissue inhibitor -1 concentration. Groups 1 (n = 5), 2 (n = 12), 3 (n = 15)

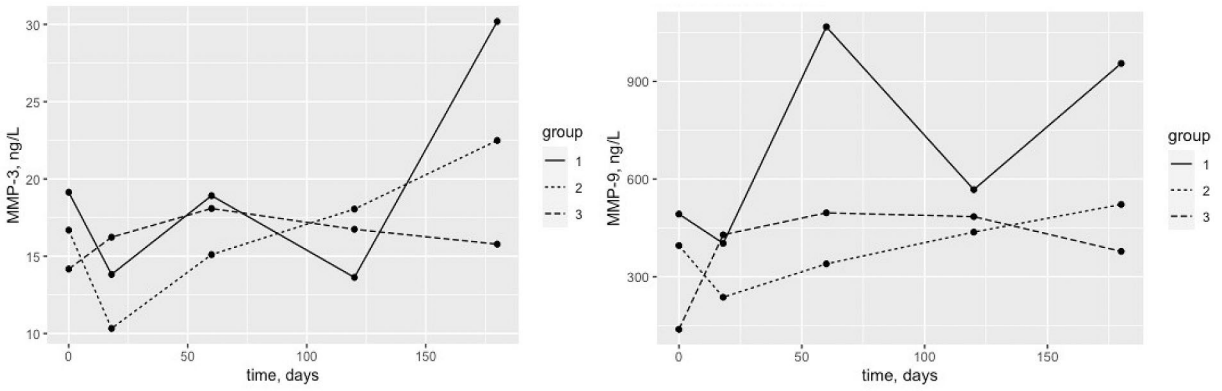

a) b)

Figure 3. Dynamics of changes in some markers associated with bone regeneration process: (a) MMP-3 concentration; (b) MMP-9 concentration. Groups 1 (*n* = 5), 2 (*n* = 12), 3 (*n* = 15).

Discussion

The results of biochemical analysis 18 days after infection in combination with positive reaction to subcutaneous immunologic test against *M. tuberculosis* (Diaskintest®) in all studied animals suggest the development of specific inflammatory process and adequacy of the used TO model. Differential changes of biochemical markers in the established observation groups are consistent with results of radiological and histological studies methods. Maintenance of specific inflammation and absence of signs of osteoregeneration by 6 months in the group 1 (infection control) was characterized by an increase in markers of nonspecific inflammation, a shifted balance of proteinase/inhibitor system towards proteolysis (MMP-9), without any and no changes in RANKL. Earlier, Kumta et al. observed an increased expression of MMP-9 in various osteolytic bone lesions and in Langerhans-type cells and found a correlation with bone destruction [26]. According to the authors, it may serve as a prognostic sign of the disease activity and progression of pathology. The growth of specific lesions with the maintaining initial level of the marker stimulating osteoclasts is probably related to the increased expression of proinflammatory cytokines, the source of which are osteoblasts infected with MBT [7], rather than the effect of RANKL [10].

The applied treatment increased bone mineralization and normalized the balance of MMP/TIMP system with a decrease in nonspecific inflammatory response. Preservation of RANKL within the reference limits during bone defects replacement may be explained by the absence of pronounced bone tissue resorption in these groups. In experimental models of osteomyelitis caused by *S. aureus* in pigs and mice, a similar lack of changes in the index was considered as its noninformativeness for monitoring the efficacy of treatment [27, 28].

The pronounced growth of ALPL in group 2 reflected a greater degree of osteogenic activity and mineralization of newly formed bone on the implant surface, and in combination with the growth of TIMP-1 suggests an earlier onset of the remodeling process in the group with autografting [19].

The use of composite material compared to autografting is characterized by slower terms of osteointegration of bone structures of the epiphyseal zone [29]. Despite this, in general, the use of biocompatible composite scaffolds has shown no negative side effects and has a number of advantages over autografts. Their use is less traumatic for the patient, as it does not require additional surgery to extract the autograft, and, unlike autografts, scaffolds can be scaled up to restore larger bone defects.

Conclusion

Tuberculous osteitis registered 18 days after infection with international standardized strain *Mycobacterium tuberculosis* H37Rv was accompanied by a significant decrease in level of peripheral blood RANKL, TIMP-1 and changes in markers of inflammatory response (ADA, NE, CP), as well as a decrease in total albumin level. At the same time, concentrations of ALPL, MMP-3 and MMP-9 did not change.

Progression of the inflammatory process by month 6 in infected untreated rabbits resulted in increased concentrations of MMP-9, decreased TIMS-1, and maintained changes in inflammatory response markers, whereas treatment promoted their normalization.

Compliance with ethical standards

All procedures involving animals complied with the ethical standards approved by the legal acts of the Russian Federation, the principles of the Basel Declaration and recommendations of the Local Ethical Committee of the Institute of Experimental Medicine.

Funding

The work was performed within the framework of State assignments of St. Petersburg Research Institute of Phthisiopulmonology of the Ministry of Health of Russian Federation (121112600145-2) and Institute of Macromolecular Compounds of Russian Academy of Sciences (124013000730-3).

Conflict of interests

The authors declare no evident and potential conflicts of interest related to the publication of this article.

References

1. Mehnath S, Sathish Kumar M, Chitra K, Jeyaraj, M. Bone-adhesive hydrogel for effective inhibition of M. tuberculosis and osteoblast regeneration. ACS Infect. Dis. 2023, 9, 2269-2281. doi: 10.1021/acsinfecdis.3c00328

2. Serdobintsev MS, Berdes, AI, Sovetova, NA, Babkov BD, Cherkasov AY. Efficacy of total hip arthroplasty in the surgical treatment of tuberculous coxitis. Meditsinskii alyans 2019; 7(4). (In Russian). doi: 10.36422/23076348-2019-7-4-86-92

3. Yi Z, Song, Q, Zhou J, Zhou Y. The efficacy of single posterior debridement, bone grafting and instrumentation for the treatment of thoracic spinal tuberculosis. Sci Rep. 2021; 11, 3591. doi: 10.1038/s41598-021-83178-0

4. Tang K, Li J, Huang T, Zhong W, Luo X, Quan Z. Clinical efficacy of three types of autogenous bone grafts in treatment of single-segment thoracic tuberculosis: A retrospective cohort study. Int J Med Sci. 2020; 17, 2844-2849. doi: 10.7150/ijms.47309

5. Wright KM, Friedland JS. Differential regulation of chemokine secretion in tuberculous and staphylococcal osteomyelitis. J Bone Miner Res. 2002; 17, 1680-1690. doi: 10.1359/jbmr.2002.17.9.1680

6. Zhang Y, Liu X, Li K, Bai, J. Mycobacterium tuberculosis 10-kDa co-chaperonin regulates the expression levels of receptor activator of nuclear factor-κB ligand and osteoprotegerin in human osteoblasts. Exp Ther Med. 2015; 9, 919-924. doi: 10.3892/etm.2014.2153

7. Takayanagi H. Osteoimmunology: shared mechanisms and crosstalk between the immune and bone systems. Nat Rev Immunol. 2007; 7, 292-304. doi: 10.1038/nri2062

8. Tobeiha M, Moghadasian MH, Amin N, Jafarnejad S. RANKL/RANK/OPG pathway: a mechanism involved in exercise-induced bone remodeling. Biomed Res Int. 2020, 2020, 1-11. doi: 10.1155/2020/6910312

9. Boyce BF, Xing L. Biology of RANK, RANKL, and osteoprotegerin. Arthritis Res Ther. 2007, 9, S1. doi: 10.1186/ar2165

10. Ma W, Jin W, He X, Sun Y, Yin H, Wang Z, Shi S. Mycobacterium tuberculosis induced osteoblast dysregulation involved in bone destruction in spinal tuberculosis. Front Cell Infect Microbiol. 2022; 12, 780272. doi: 10.3389/fcimb.2022.780272

11. Krane SM, Inada M. Matrix metalloproteinases and bone. Bone. 2008; 43, 7-18. doi: 10.1016/j.bone.2008.03.020

12. Cassuto J, Folestad A, Göthlin J, Malchau H, Kärrholm J. Concerted actions by MMPs, ADAMTS and serine proteases during remodeling of the cartilage callus into bone during osseointegration of hip implants. Bone Reports. 2020; 13, 100715. doi: 10.1016/j.bonr.2020.100715

13. Ren L-R, Wang H, He X-Q, Song M-G, Chen X-Q, Xu Y-Q. Staphylococcus aureus Protein A induces osteoclastogenesis via the NF-κB signaling pathway. Mol Med Rep. 2017; 16, 6020-6028. doi: 10.3892/mmr.2017.7316

14. Paiva KBS, Granjeiro JM. Bone tissue remodeling and development: Focus on matrix metalloproteinase functions. Arch Biochem Biophys. 2014; 561, 74-87. doi: 10.1016/j.abb.2014.07.034

15. Liang HPH, Xu J, Xue M, Jackson C. Matrix metalloproteinases in bone development and pathology: current knowledge and potential clinical utility. Met Med. 2016; 3, 93-102. doi: 10.2147/MNM.S92187

16. Sabir N, Hussain T, Mangi MH, Zhao D, Zhou X. Matrix metalloproteinases: Expression, regulation and role in the immunopathology of tuberculosis. Cell Prolif. 2019, 52, e12649. doi: 10.1111/cpr.12649

17. Shubayev VI, Branemark R, Steinauer J, Myers RR. Titanium implants induce expression of matrix metalloproteinases in bone during osseointegration. J Rehabil Res Dev. 2004, 41, 757. doi: 10.1682/JRRD.2003.07.0107

18. Stepanova M, Averianov I, Serdobintsev M, Gofman I, Blum N, Semenova N, Nashchekina Y, Vinogradova T, Korzhikov-Vlakh V, Karttunen M, et al. PGlu-modified nanocrystalline cellulose improves mechanical properties, biocompatibility, and mineralization of polyester-based composites. Materials (Basel). 2019; 12, 3435. doi: 10.3390/ma12203435

19. Averianov I, Stepanova M, Solomakha O, Gofman I, Serdobintsev M, Blum N, Kaftuirev A, Baulin I, Nashchekina J, Lavrentieva A, et al. 3D-Printed composite scaffolds based on poly(ε-caprolactone) filled with poly(glutamic acid)-modified cellulose nanocrystals for improved bone tissue regeneration. J Biomed Mater Res. Part B Appl. Biomater. 2022, 110, 2422-2437. doi: 10.1002/jbm.b.35100

20. Vinogradova TI, Serdobintsev MS, Korzhikova-Vlakh EG, Korzhikov-Vlakh VA, Kaftyrev AS, Blum NM, Semenova NY, Esmedlyaeva DS, Dyakova ME, Nashchekina, YA, et al. Comparison of autografts and biodegradable 3D-printed composite scaffolds with osteoconductive properties for tissue regeneration in bone tuberculosis. Biomedicines. 2023, 11, 2229. doi: 10.3390/biomedicines11082229

21. Vasilyeva SN, Kaftyrev AS, Vinogradova TI, Serdobintsev MS, Zabolotnykh NM. A method for modeling tuberculous ostitis of varying severity. 2011, Patent RU 2421823 C1. (In Russian).

22. Visser L, Blout ER. The use of p-nitrophenyl N-tert-butyloxycarbonyl-L-alaninate as substrate for elastase. Biochim Biophys Acta (Enzymology). 1972, 268, 257-260. doi: 10.1016/0005-2744(72)90223-9

23. Giusti G. Adenosine deaminase. In Methods of Enzymatic Analysis; (Bergmeyer HU, Ed). Academic Press: New York, NY, 1974 pp. 1092-1099.

24. Alexeyeva N. Dual balance correction in repeated measures Anova with missing data. Electronic J Appl Stat Analysis. 2017, 10 (1), 146-159. doi: 10.1285/i20705948v10n1p146

25. Gaifullin N. Cellular mechanisms of bone remodeling due to external overload and to the conditions of titan implant osseointegration. Vestn Volgogr State Univ. Ser. 11. 2016, 6, 16-25. (In Russian). doi: 10.15688/jvolsu11.2016.1.2

26. Kumta SM, Huang L, Cheng YY, Chow LTC, Lee KM, Zheng MH. Expression of VEGF and MMP-9 in giant cell tumor of bone and other osteolytic lesions. Life Sci. 2003; 73, 1427-1436. doi: 10.1016/s0024-3205(03)00434-x

27. Granata V, Possetti V, Parente R, Bottazzi B, Inforzato A, Sobacchi C. The osteoblast secretome in Staphylococcus aureus osteomyelitis. Front Immunol. 2022; 13, 1048505. doi: 10.3389/fimmu.2022.1048505

28. Şen H. Plasma RANKL level is not a reliable marker to monitor the bone destruction in mice model of osteomyelitis. J Dis Relat Surg 2022; 33, 193-202. doi: 10.52312/jdrs.2022.537

29. Xu Z, Wang N, Ma Y, Dai H, Han B. Preparation and study of 3D printed dipyridamole/β-tricalcium phosphate/polyvinyl alcohol composite scaffolds in bone tissue engineering. J Drug Deliv Sci Technol. 2022; 68, 103053. doi: 10.1016/j.jddst.2021.103053

Динамика показателей системы матриксных металлопротеиназ и их ингибиторов в крови в лечении экспериментального туберкулезного остита

Диляра С. Эсмедляева [1], Нина П. Алексеева [2], Марина Е. Дьякова [1], Наталья Ю. Семенова [3], Виктор А. Коржиков-Влах [2], Евгения Г. Коржикова-Влах [4], Татьяна И. Виноградова [1], Петр К. Яблонский [1,2]

[1] ФГБУ «Санкт-Петербургский научно-исследовательский институт фтизиопульмонологии» Минздрава России, Санкт-Петербург, Россия

[2] ФГБОУВО «Санкт-Петербургский государственный университет», Санкт-Петербург, Россия

[3] ФГБУ «Российский научно-исследовательский гематологии и трансфузиологии» ФМБА, Санкт-Петербург, Россия

[4] ФГБУ Институт высокомолекулярных соединений Российской академии наук, Санкт-Петербург, Россия

Резюме

Дисбаланс костного гомеостаза связан с нарушениями в сигнальной системе рецептор-активатор ядерного фактора-κB RANK/RANKL/остеопротегерин (OPG), опосредованный действием матриксных металлопротеиназ (MMP). Целью данной работы являлась оценка динамики показателей системы (MMP)/ингибиторы в крови при развитии туберкулезного остита (ТО) в различных группах (n = 32): инфекционный контроль (группа 1) и две экспериментальные группы, в которых последовательно проводились некрэктомия, противотуберкулезное лечение и пластические операции с использованием аутотрансплантатов (группа 2) или 3D-печатных композитных скаффолдов (группа 3). В крови определяли уровень MMP-3 и MMP-9, их тканевого ингибитора (TIMP-1), лиганда активатора рецептора ядерного фактора-κB (RANKL), неспецифической щелочной фосфатазы (ALPL), альбумина (AL), церулоплазмина (CP), нейтрофильной эластазы (NE) и аденозиндезаминазы (ADA) до заражения и через 18 дней, 2, 4 и 6 месяцев после заражения. Остеогенез оценивали по результатам микрокомпьютерной томографии и гистологического исследования костной ткани в контрольной и опытных группах. На этапе верификации туберкулезного остита выявлено снижение RANKL (p = 0,017) и AL (p = 0,04), повышение TIMP-1 (p = 0,04), CP (p = 0,0004) и EL (p = 0,02), при отсутствии изменений ALPL, ADA, а также MMP-3 и MMP-9. В группе 1 (инфекционный контроль) сохранялись очаги специфического повреждения и не было выявлено признаков остеорегенерации. В обеих экспериментальных группах наблюдалась прогрессирующая регенерация костной ткани, при этом наименьшее количество баллов за остеодеструкцию было отмечено в группе 2 (аутотрансплантация). Уровень воспалительной реакции увеличивался по мере прогрессирования инфекции и снижался по мере лечения. Уровень RANKL не изменялся в период от 2 до 6 месяцев. Исходя из различий в показателях ALPL и TIMP-1, использование композитного материала для пластической хирургии характеризовалось более медленным остеоинтеграцией и репаративным остеогенезом по сравнению с использованием аутотрансплантата.

Ключевые слова

Костный туберкулез, матриксные металлопротеиназы, аутотрансплантация, биокомпозитные скаффолды, пластическая хирургия, биоматериалы, регенерация костей.